UDC 004.94 http://dx.doi.org/10.30970/vam.2024.34.00000

IMPROVED BOUNDARY SAMPLING TECHNIQUES FOR SMOOTHED PARTICLE HYDRODYNAMICS WITH RIGID BODY COUPLING

O. Hrytsyshyn, V. Trushevskyy

Ivan Franko National University of Lviv,
1, Universytetska str., 79000, Lviv, Ukraine,
e-mail: ostap.hrytsyshyn@lnu.edu.ua, valeriy.trushevsky@lnu.edu.ua

A practical approach for fluid–rigid interaction in Smoothed Particle Hydrodynamics (SPH) is introduced. It keeps only one boundary layer and assigns each boundary particle a volume–corrected effective mass. Multi–layer boundaries can be accurate, but in practice they are heavy: neighbor lists grow, interaction counts rise, and many wall samples do redundant work. The single–layer idea stays on the rigid surface and compensates missing neighbors by a local volume estimate V_b, mapped to $\hat{m}_b = \rho_0 V_b$. With this correction, density and pressure sums near the wall remain consistent even for thin plates and shells, while the number of pairwise interactions goes down.

The coupling uses standard symmetric SPH forces, so linear and angular momentum are preserved without contact penalties or position corrections. Integration is straightforward in both WCSPH (Weakly compressible SPH) and PCISPH (Predictive–corrective incompressible SPH): only the density summation receives the extra boundary terms, whereas pressure and viscous parts keep their usual form. The scheme is friendly to implementation, works with existing neighbor search, and allows slip control through common viscosity parameters.

Key words: smoothed Particle Hydrodynamics (SPH), fluid–rigid coupling, boundary sampling, single–layer boundary, volume correction, particle deficiency, real–time simulation.

1. Introduction

Smoothed Particle Hydrodynamics (SPH) is a mesh–free method where fields are approximated by local sums over neighbors with a smoothing kernel. The early idea comes from astrophysics [1]. In graphics and engineering, two popular choices are WCSPH (Weakly compressible SPH) and PCISPH (Predictive-corrective incompressible SPH), mainly because they are simple and fast for many incompressible scenes [2, 3].

When rigid bodies are introduced into the fluid, behavior becomes more sensitive near walls. If the kernel support is not fully filled, fluid particles close to a boundary lose neighbors. Then density is underestimated and pressure gets noisy. It may lead to sticking or even small penetrations. Different boundary models try to fix this: frozen or ghost particles, penalty/contact forces, and particle boundaries sampled on the surface [4, 6]. Each model has benefits and costs.

Complementary to our previous IISPH study, where we implemented and validated an incompressible SPH solver on the Taylor–Green vortex benchmark [7], this paper focuses on boundary sampling and two–way rigid–fluid coupling; the proposed single–layer scheme integrates with WCSPH/PCISPH without additional forces or position corrections.

In production code, stable two–way coupling and speed are important. Particle boundaries are attractive because they match SPH formulas and give symmetric forces with the rigid body. But a common recommendation is to place several boundary layers to fill the kernel radius. Accuracy is good, but cost grows fast with each extra layer. The aim is to keep cost low and still have smooth density and pressure next to the wall.

2. Problem statement

The fluid is single-phase and Newtonian; surface tension and multiphase effects are not considered. Flows are low-Mach for WCSPH and near-incompressible for PCISPH. Rigid bodies are treated as perfectly rigid with six-degree-of-freedom motion and exchange linear/angular momentum with the fluid only via particle interactions at the interface. The method targets moderate Reynolds numbers typical for graphics and real-time engineering scenarios.

The goal is to design a boundary sampling and weighting scheme that: (i) uses a *single* layer of boundary particles placed on the rigid surface, (ii) yields unbiased density and stable pressures for fluid particles near walls, (iii) preserves pairwise force symmetry for momentum conservation, (iv) drops into both WCSPH and PCISPH without extra solver passes, contact penalties, or position corrections, and (v) reduces the number of fluid–boundary pair evaluations (and thus cost) for a fixed fluid resolution.

Typical use-cases include free-surface flows in tanks and channels with immersed rigid obstacles (thin plates, shells, rods), stirrer-like bodies, and moving mechanisms submerged in liquid. In all cases the interaction is localized to the fluid–solid interface.

Effectiveness is judged by (a) density/pressure smoothness near the wall, (b) absence of sticking/penetration, and (c) reduced interaction counts and/or runtime at comparable accuracy.

A single layer of boundary particles is placed directly on the rigid surface, and each boundary particle is assigned a volume that it represents on the surface. Based on this volume, its effective mass is scaled in density and pressure computations. In this way, missing neighbors are compensated in the sums. The interaction then uses the usual symmetric pressure and viscous terms known from WCSPH and PCISPH [2, 3]. In practice this keeps densities smooth near the wall and reduces interaction counts, while the implementation stays small.

3. Background and Related Work

This section gives short background and connects to related work used later. Notation is kept simple and close to common SPH papers.

A field A at particle i with neighbors j is approximated using the smoothing kernel $W_{ij} = W(\mathbf{x}_i - \mathbf{x}_j, h)$:

$$A(\mathbf{x}_i) \;\approx\; \sum_j A_j \,\frac{m_j}{\rho_j}\, W_{ij}. \tag{1}$$

The standard density summation is

$$\rho_i \;=\; \sum_j m_j\, W_{ij}. \tag{2}$$

For incompressible flows two popular choices exist. In WCSPH, pressure is computed from a simple state equation and then symmetric forces are applied [3]:

$$p_i \;=\; c^2\,(\rho_i - \rho_0), \qquad \mathbf{a}_i^p \;=\; -\sum_j m_j \left(\frac{p_i}{\rho_i^2} + \frac{p_j}{\rho_j^2}\right) \nabla W_{ij}. \tag{3}$$

Here c is the artificial speed of sound and ρ_0 is the rest density. PCISPH instead iteratively corrects the pressure so that density error becomes small while keeping similar

symmetric form for forces [2].

Close to a wall, fluid particles lose neighbors inside the kernel support. Then (2) underestimates ρ_i and (3) gives noisy p_i. Different models try to fix this. Particle boundaries sampled on the surface are attractive because they fit (1) and keep symmetry of forces. Monaghan's particle boundary forces treat general shapes [6]. Ihmsen et al. discuss boundary handling for PCISPH and show how missing neighbors near walls cause sticking or pressure jumps if not treated carefully [4]. Constraint-based fluids give another angle, where constraints help to control incompressibility and contact, but they are heavier to integrate into a simple SPH code path [5].

For two–way coupling the goal is the same pairwise symmetry as in (3) so that linear and angular momentum are conserved between fluid and rigid body. In practice the pressure part dominates the exchange; the viscous part adds drag and controls slip. WCSPH [3] and PCISPH [2] both work with particle boundaries, but they are sensitive to how the wall is sampled because the sums in (1) and (2) expect the kernel to be well "filled".

Multi–layer boundary sampling fills the kernel, but cost grows fast with each extra layer. Single–layer sampling is cheap and easy to prepare, yet it suffers from particle deficiency: boundary contributions in (1) and (2) are too small, so the fluid near the wall gets biased density and pressure. Prior works add special forces or extra corrections [4, 6], which increases complexity. A simpler alternative is to keep one boundary layer, estimate the represented boundary volume, and scale its contribution by a corrected mass

$$\hat{m}_b \;=\; \rho_0\, V_b, \tag{4}$$

so that standard SPH sums recover the "missing" neighbors without new force terms. Here $\hat{m}_b$ is the *effective* mass assigned to boundary particle b; ρ_0 is the fluid rest density from (3); and V_b is the small volume of solid represented by particle b. The volume V_b is determined from the local boundary sampling density, becoming smaller in densely sampled regions and larger in sparse ones.

4. Preliminaries and Notation

This section sets the notation for later parts and recalls basic SPH facts needed by the method. Notation is kept simple and compact. Equations (1)–(3) from Section 2 serve as the base formulas.

Let $W(\mathbf{r}, h)$ be the smoothing kernel with length scale h and relative vector $\mathbf{r} = \mathbf{x}_i - \mathbf{x}_j$. Normalization and compact support are

$$\int_{\mathbb{R}^d} W(\mathbf{r}, h)\, d\mathbf{r} = 1, \qquad W(\mathbf{r}, h) = 0 \text{ for } \|\mathbf{r}\| \geq r_{\text{supp}}. \tag{5}$$

Symmetry implies antisymmetry for the gradient,

$$W(\mathbf{r}, h) = W(-\mathbf{r}, h), \qquad \nabla_i W(\mathbf{x}_i - \mathbf{x}_j, h) = -\nabla_j W(\mathbf{x}_j - \mathbf{x}_i, h). \tag{6}$$

For a well sampled neighborhood, the discrete 0th- and 1st-order consistency conditions read

$$\sum_j \frac{m_j}{\rho_j} W_{ij} \approx 1, \tag{7}$$

$$\sum_j \frac{m_j}{\rho_j} (\mathbf{x}_j - \mathbf{x}_i) W_{ij} \approx \mathbf{0}. \tag{8}$$

When (7)–(8) hold, interpolation (1) is unbiased to first order. The popular cubic spline kernel satisfies (5)–(6) and is used in experiments, but the derivations do not depend on a specific kernel.

Density is computed by the standard sum (2). In WCSPH, pressure follows the state relation (3) [3], while PCISPH predicts and corrects pressure iteratively to drive the density error to a small value [2]. In both cases, the symmetric pressure acceleration has the form already shown in (3) and guarantees momentum conservation for particle pairs.

Laminar artificial viscosity is used for dissipation and simple slip control. For fluid–fluid pairs (i, j) it is convenient to define

$$\Pi_{ij} \;=\; -\,\nu\,\frac{\min\big(\mathbf{v}_{ij}\cdot\mathbf{x}_{ij},\,0\big)}{\|\mathbf{x}_{ij}\|^2+\varepsilon h^2}, \qquad \nu \;=\; \frac{2\,\alpha\,h\,c}{\rho_i+\rho_j}, \quad \varepsilon=10^{-2}, \tag{9}$$

with $\mathbf{v}_{ij}=\mathbf{v}_i-\mathbf{v}_j$ and $\mathbf{x}_{ij}=\mathbf{x}_i-\mathbf{x}_j$ [3]. The corresponding viscous acceleration is

$$\mathbf{a}_i^{\nu} \;=\; -\sum_j m_j\,\Pi_{ij}\,\nabla W_{ij}. \tag{10}$$

Parameters α and c are shared with WCSPH/PCISPH settings from (3). These choices are standard in graphics and give robust behavior for moderate Reynolds numbers.

Near a wall, the kernel support is truncated and the sums in (2) and (3) lose neighbors on the boundary side. Two small diagnostics help to detect this situation in a solver:

First, the normalization deficit,

$$e_i^{(0)} \;=\; \left|\,1-\sum_j \frac{m_j}{\rho_j}\,W_{ij}\right|, \tag{11}$$

which should be close to zero when the neighborhood is well filled. Second, the first-moment residual,

$$e_i^{(1)} \;=\; \left\|\sum_j \frac{m_j}{\rho_j}\,(\mathbf{x}_j-\mathbf{x}_i)\,W_{ij}\right\|, \tag{12}$$

which should be small for a roughly symmetric neighbor distribution. Large values of (11) or (12) mark particle deficiency and often correlate with noisy pressures from (3).

The single-layer boundary model addresses this by adding boundary contributions that use a corrected mass $\hat{m}_b$ as in (4). In Section 4, the corrected density and force terms will be written so that (7) is approximately restored close to the wall and (11)–(12) are reduced in practice [4, 6].

5. Method: Single–Layer Boundary Sampling with Volume–Corrected Mass

This section presents the concrete boundary sampling on the rigid surface and the formulas used later in the solver. The plan is to keep one boundary layer and compensate missing neighbors by a local volume and a corrected mass. Interpolation (1), density sum (2), and the symmetric pressure term from (3) stay unchanged for fluid–fluid pairs.

The rigid surface is sampled by a single layer of boundary particles with spacing close to the fluid particle spacing. Let $\mathcal{B}$ be the set of boundary particles. Only boundary particles that have at least one fluid neighbor inside the kernel support are considered

active in a time step to save cost [4]. For compact notation, $\mathcal{F}(i)$ and $\mathcal{B}(i)$ denote fluid and boundary neighbors of a fluid particle i.

A boundary particle represents a small portion of solid volume around the surface. This portion is estimated by the local boundary sampling density

$$\delta_b \;=\; \sum_{k\in\mathcal{B}(b)} W(\mathbf{x}_b - \mathbf{x}_k, h). \tag{13}$$

Assuming equal boundary masses in the layer, the represented volume becomes

$$V_b \;\approx\; \frac{1}{\delta_b}. \tag{14}$$

Using the fluid rest density from (3), the corrected boundary mass follows from (4) as $\hat{m}_b = \rho_0 V_b$. In dense regions δ_b is larger and V_b becomes smaller; in sparse regions V_b grows and compensates the missing neighbors.

The density estimate of a fluid particle near a wall is extended by boundary contributions that use the corrected mass:

$$\rho_i \;=\; \sum_{j\in\mathcal{F}(i)} m_j\, W_{ij} \;+\; \sum_{b\in\mathcal{B}(i)} \hat{m}_b\, W_{ib}. \tag{15}$$

The first term equals the standard density sum (2), while the second term restores the missing mass from the wall side. With (15), the state relation in (3) produces smoother pressures next to the boundary.

Pressure exchange with the wall keeps the symmetric SPH form but replaces the neighbor mass by the corrected boundary mass. The acceleration of a fluid particle due to pressure from boundary neighbors is

$$\mathbf{a}_i^{p|\mathcal{B}} \;=\; -\sum_{b\in\mathcal{B}(i)} \hat{m}_b \left(\frac{p_i}{\rho_i^2}\right) \nabla W_{ib}. \tag{16}$$

This follows the idea used in particle boundary forces [4, 6] but stays consistent with the symmetric term of (3). Equal and opposite forces are applied to the rigid body through its boundary particles, so momentum is conserved.

Slip control and drag are added with a laminar artificial viscosity acting between fluid and boundary neighbors, similar in spirit to (9) but using the boundary mass correction:

$$\Pi_{ib} \;=\; -\nu\, \frac{\min(\mathbf{v}_{ib}\cdot\mathbf{x}_{ib},\, 0)}{\|\mathbf{x}_{ib}\|^2 + \varepsilon h^2}, \qquad \nu \;=\; \frac{2\,\alpha\, h\, c}{\rho_i + \rho_0}, \quad \varepsilon = 10^{-2}, \tag{17}$$

with $\mathbf{v}_{ib} = \mathbf{v}_i - \mathbf{v}_b$ and $\mathbf{x}_{ib} = \mathbf{x}_i - \mathbf{x}_b$. The boundary contribution to viscous acceleration is then

$$\mathbf{a}_i^{\nu|\mathcal{B}} \;=\; -\sum_{b\in\mathcal{B}(i)} \hat{m}_b\, \Pi_{ib}\, \nabla W_{ib}. \tag{18}$$

Parameter α controls slip: $\alpha = 0$ gives almost free slip; larger α increases tangential drag [3].

Because V_b adapts to local sampling through (14), the single-layer model stays stable on thin plates, rods, and non–manifold junctions. Dense areas contribute less due to smaller V_b; sparse areas contribute more. As a result, density (15) and forces (16)–(18) remain consistent without extra layers or position correction [4].

6. Two–Way Coupling Forces

This section defines the forces exchanged between fluid and rigid through boundary particles. The pairwise form keeps symmetry and uses the corrected boundary mass from (4) together with the kernel interactions already used in (16) and (18). Momentum conservation then follows directly from action–reaction pairs [4, 6].

For a fluid particle i and a boundary particle b, the pairwise pressure force applied *to the fluid* is written from the acceleration in (16) as

$$\mathbf{f}^{p}_{i\leftarrow b} \;=\; m_i\,\mathbf{a}_i^{p|b} \;=\; -\,m_i\,\hat{m}_b\left(\frac{p_i}{\rho_i^2}\right)\nabla W_{ib}. \tag{19}$$

The boundary particle receives the opposite reaction,

$$\mathbf{f}^{p}_{b\leftarrow i} \;=\; -\,\mathbf{f}^{p}_{i\leftarrow b}. \tag{20}$$

Equations (19)–(20) are consistent with symmetric SPH pressure forms and use only the fluid state (p_i, ρ_i) on the right, which is standard for particle boundaries [4, 6]. As density near the wall is stabilized by (15), the pressure from (3) grows smoothly with compression and prevents penetration without extra position correction.

Tangential drag and slip control follow the laminar artificial viscosity. Using Π_{ib} from (17), the pairwise viscous force *to the fluid* is

$$\mathbf{f}^{\nu}_{i\leftarrow b} \;=\; -\,m_i\,\hat{m}_b\,\Pi_{ib}\,\nabla W_{ib}, \tag{21}$$

and the reaction on the boundary particle is

$$\mathbf{f}^{\nu}_{b\leftarrow i} \;=\; -\,\mathbf{f}^{\nu}_{i\leftarrow b}. \tag{22}$$

The parameter α in (17) sets the effective slip: small α produces almost free slip, while larger values increase drag along the surface [3]. The same form is used for WCSPH and PCISPH [2].

For every interacting pair (i, b) the pressure and viscous forces satisfy

$$\mathbf{f}^{p}_{i\leftarrow b} + \mathbf{f}^{p}_{b\leftarrow i} = \mathbf{0}, \qquad \mathbf{f}^{\nu}_{i\leftarrow b} + \mathbf{f}^{\nu}_{b\leftarrow i} = \mathbf{0}. \tag{23}$$

Summing (23) over all pairs gives zero net internal force, so linear and angular momentum are conserved by construction. This is the key advantage of particle boundaries with symmetric forms [6].

The total force on a boundary particle from nearby fluid particles is

$$\mathbf{f}_b \;=\; \sum_{i\in\mathcal{F}(b)} \Big(\mathbf{f}^{p}_{b\leftarrow i} + \mathbf{f}^{\nu}_{b\leftarrow i}\Big). \tag{24}$$

For a rigid body with boundary set $\mathcal{B}_r$ and center of mass $\mathbf{x}_{\mathrm{cm}}$, the net force and torque are

$$\mathbf{F}_{\mathrm{rigid}} \;=\; \sum_{b\in\mathcal{B}_r} \mathbf{f}_b, \qquad \boldsymbol{\tau}_{\mathrm{rigid}} \;=\; \sum_{b\in\mathcal{B}_r} (\mathbf{x}_b - \mathbf{x}_{\mathrm{cm}}) \times \mathbf{f}_b. \tag{25}$$

These quantities are passed to the rigid-body solver at each step. No boundary normals are required, and multiple contacts are handled naturally since (24) is local per boundary particle [4].

Stable behavior depends on three simple conditions. The density near walls should be computed with (15) so that (3) gives consistent pressures. The viscosity parameters in (17) should respect the time-step limits in Section 3 to avoid oversmoothing. Finally, the corrected mass $\hat{m}_b$ should be updated from (14) when boundary sampling density changes, for example during contacts or fast motion [4].

7. Solver Integration

This section shows how the boundary model is inserted into a standard SPH loop. The order is: synchronize the rigid state, activate nearby boundary particles, evaluate densities and pressures, assemble two–way forces, and integrate in time. Formulas from Sections 2–5 are reused without modification.

Rigid transforms are applied to boundary particle positions $\mathbf{x}_b$ at the beginning of the step. A neighbor search is then executed for all fluid particles. A boundary particle becomes *active* if at least one fluid particle is inside its kernel support; this is expressed by the indicator

$$\chi_b \;=\; \begin{cases} 1, & \exists\, i \text{ s.t. } \|\mathbf{x}_b - \mathbf{x}_i\| < r_{\mathrm{supp}}, \\ 0, & \text{otherwise.} \end{cases} \tag{26}$$

Only active boundary particles take part in the following computations. For each active b, the local boundary sampling density δ_b is computed by (13), the represented volume V_b by (14), and the corrected mass $\hat{m}_b = \rho_0 V_b$ by (4). Processing only particles with $\chi_b = 1$ keeps the overhead proportional to the effective contact area [4].

Fluid density employs the extended summation

$$\rho_i \;=\; \sum_{j\in\mathcal{F}(i)} m_j\, W_{ij} \;+\; \sum_{b\in\mathcal{B}(i)} \hat{m}_b\, W_{ib}, \tag{27}$$

which is identical to (15) and repeated here for completeness of the solver description. In WCSPH, pressure follows the equation of state (3) [3]. In PCISPH, the same density estimate (27) is used inside the pressure correction loop until the target density error is met [2]. The corrected boundary mass $\hat{m}_b$ removes the typical underestimation of ρ_i close to walls and avoids noisy p_i values [4, 6].

Fluid–fluid pressure uses the standard symmetric form

$$\mathbf{a}_i^{p|\mathcal{F}} \;=\; -\sum_{j\in\mathcal{F}(i)} m_j \left(\frac{p_i}{\rho_i^2} + \frac{p_j}{\rho_j^2}\right) \nabla W_{ij}, \tag{28}$$

and fluid–boundary pressure uses (16). Viscous terms combine the fluid–fluid contribution (10) with the fluid–boundary contribution (18). External accelerations (e.g., gravity) are then added. The total acceleration becomes

$$\mathbf{a}_i \;=\; \mathbf{a}_i^{p|\mathcal{F}} + \mathbf{a}_i^{p|\mathcal{B}} + \mathbf{a}_i^{\nu} + \mathbf{a}_i^{\nu|\mathcal{B}} + \mathbf{a}_i^{\mathrm{ext}}. \tag{29}$$

On the rigid side, action–reaction pairs from Section 5 are accumulated per boundary particle and converted to forces and torques by (24)–(25). This keeps momentum conservation without normals or penetration constraints [4, 6].

The step size follows standard WCSPH/PCISPH limits [2–4]. First, a CFL-like bound and a viscous bound are computed,

$$\Delta t_{\mathrm{cfl}} \;=\; C_{\mathrm{cfl}}\, \frac{h}{c + \max_i \|\mathbf{v}_i\|}, \tag{30}$$

$$\Delta t_\nu \;=\; C_\nu \,\frac{h^2}{\max(\nu_i)}, \qquad \nu_i \text{ from (9) or (17).} \tag{31}$$

The step size is then chosen as

$$\Delta t \;=\; \min\big(\Delta t_{\mathrm{cfl}},\, \Delta t_\nu\big), \tag{32}$$

with safety factors $C_{\mathrm{cfl}}, C_\nu \in [0.2, 0.4]$. For PCISPH, (32) defines the predictor step; several pressure corrections are performed inside the step until the density error target is reached [2]. States are advanced explicitly,

$$\mathbf{v}_i^{t+\Delta t} \;=\; \mathbf{v}_i^{t} + \Delta t\, \mathbf{a}_i, \qquad \mathbf{x}_i^{t+\Delta t} \;=\; \mathbf{x}_i^{t} + \Delta t\, \mathbf{v}_i^{t+\Delta t}. \tag{33}$$

Before the next step, neighbors and the activation mask (26) are rebuilt to avoid tunneling of fast moving boundaries [4].

The dominant cost remains the neighbor search and pressure evaluation. Activating only boundary particles with $\chi_b = 1$ limits overhead. Volumes V_b adapt to the local sampling density via (14), so thin plates, rods, and non–manifold junctions behave stably without extra layers. When contact patterns change, δ_b, V_b, and $\hat{m}_b$ are recomputed before evaluating (27) and the forces, keeping density and pressure smooth across time [4].

8. Results

This section evaluates the proposed single–layer boundary with volume–corrected mass on a fixed benchmark scene and reports interaction counts together with qualitative stability observations.

The benchmark is a two–dimensional rectangular tank with static outer walls (left, right, bottom, top). Inside the tank, five rigid bodies are present: four rectangular boxes and one sphere. All five interior bodies are treated as *dynamic* rigid bodies (they receive and apply two–way forces), whereas the tank walls are *static* boundaries.

The boxes are initially resting on the bottom and arranged as in Fig. 1. The sphere starts above the free surface at mid–width and is released from rest at $t = 0$ under gravity, producing a crater, side jets, and a central splash upon impact. Color in the frames corresponds to velocity of fluid particles (blue $\to$ low, red $\to$ high).

A reference scene was simulated for 24 steps with 20,000 fluid particles. Two boundary samplings were compared: a multi–layer discretization with 14,272 boundary particles and a single–layer discretization with 3,032 boundary particles. Both runs used the same fluid settings and the same rigid motion. The single–layer variant employed the density extension in (15) together with the corrected mass $\hat{m}_b = \rho_0 V_b$ from (4).

Across all frames, the total number of fluid–boundary interactions was lower for the single–layer case. The multi–layer configuration produced on average about 18,032 interactions per step, while the single–layer case produced about 13,958. This is a reduction of roughly 4,074 interactions per step, i.e. about 22.6% fewer pair evaluations for the same fluid state. Fig. 2 summarizes the trend.

When normalized per fluid particle, the interaction rate was around 0.90 for the multi–layer and 0.70 for the single–layer sampling. When normalized per boundary particle, the difference is stronger: each boundary particle in the single–layer setup contributed on average to more than 4.6 interactions, while in the multi–layer case the value was about 1.26. This shows that multi–layer sampling tends to oversample the wall region and triggers redundant computations that do not change the flow noticeably.

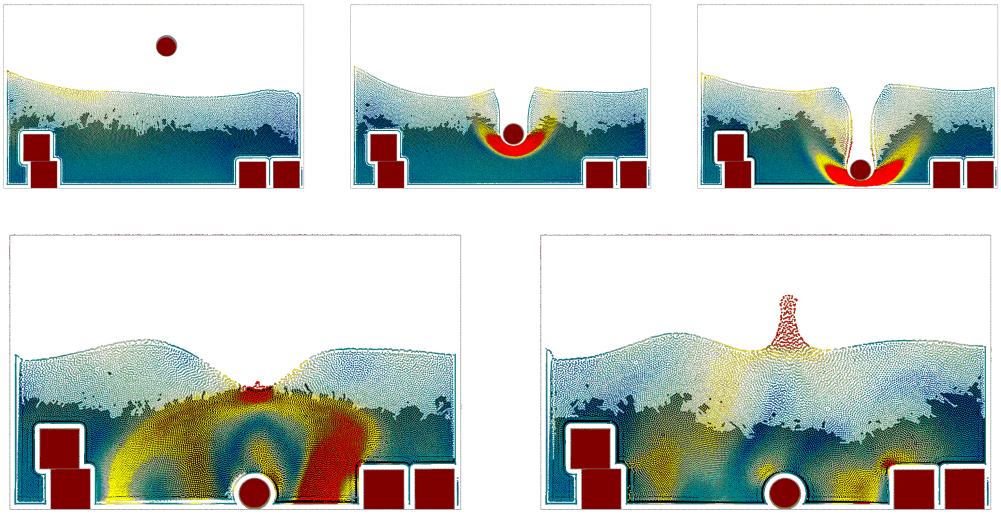

Fig. 1. Benchmark snapshots (left-to-right, top-to-bottom): The sphere falls into the fluid and generates a cavity, plunging jet, and subsequent rebound. Colors indicate velocity. Container walls are static throughout

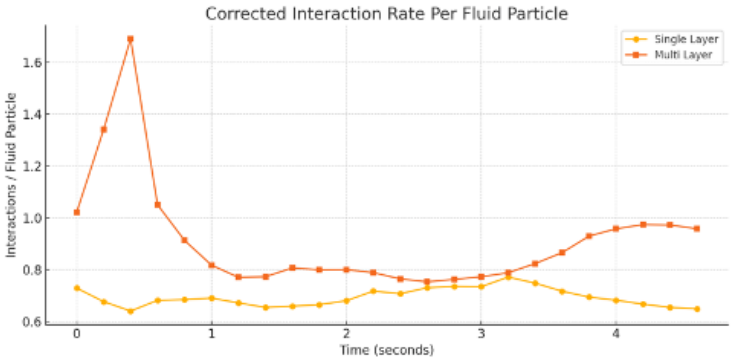

Fig. 2. Interaction rate over time for single–layer and multi–layer boundary samplings. Lower curve corresponds to the single–layer setup

Without the mass correction, a single layer near thin plates, shells, or rods would suffer from particle deficiency: the kernel support is not filled and density close to the wall is underestimated. With the corrected contribution $\hat{m}_b = \rho_0 V_b$ and the extended density sum (15), this deficiency is compensated. In the tested scene, the pressure field near walls stayed smooth and penetration was not observed, even for lower–dimensional shapes. The model therefore allows simpler and cheaper boundary representations while keeping the same symmetric force exchange used in Section 6

9. Conclusions

The paper presented a compact boundary model for SPH that uses a *single* particle layer on rigid surfaces together with a volume–corrected boundary mass. The correction

is expressed by $\hat{m}_b = \rho_0 V_b$ in (4), where V_b adapts to the local sampling density. With this choice, the extended density sum (15) restores the missing support close to walls, while pressure and viscous exchanges keep the standard symmetric pairwise form, see (19)–(22). The method integrates directly into WCSPH and PCISPH loops without extra position corrections or special boundary forces.

Experiments with 20,000 fluid particles showed that the single–layer sampling with volume correction reduces the total number of fluid–boundary interactions by about 22.6% compared to a multi–layer discretization (on average 13,958 vs. 18,032 pairs per step), see Figure 2. Normalized per fluid particle, rates were roughly 0.70 (single layer) vs. 0.90 (multi layer). Normalized per boundary particle, the single layer was much more efficient (≈ 4.6 vs. 1.26 interactions on average). At the same time, density and pressure near walls stayed smooth; sticking and small penetrations were not observed in the tested scene.

From an implementation view, the model stays light. Only boundary particles that are close to the fluid are activated each step, their local sampling δ_b is evaluated by (13), and the represented volume V_b by (14). Forces are then accumulated with (24)–(25) to drive the rigid solver. No boundary normals are required, and thin plates, rods, or non–manifold junctions are handled naturally because V_b adapts to the local sampling.

There are still limits. The minimal thickness that can be represented is tied to the fluid particle scale; extremely compressible flows were not addressed; very fast motions need the standard SPH time–step control of Section 3 to avoid tunneling. Future work can include adaptive boundary sampling (coarser in flat regions, denser in high curvature), coupling with measured wall roughness for better slip control through the α parameter in (17), and validation on multi–phase scenes and higher Reynolds numbers. Despite these open points, the volume–corrected single layer offers a simple, robust, and efficient option for two–way rigid–fluid coupling.

References

1. Gingold R.A. Smoothed particle hydrodynamics: theory and application to non-spherical stars / R.A. Gingold, J.J. Monaghan // Monthly Notices of the Royal Astronomical Society. – 1977. – Vol. 181, № 3. – P. 375–389.
2. Solenthaler B. Predictive-corrective incompressible SPH / B. Solenthaler, R. Pajarola // ACM Transactions on Graphics (SIGGRAPH Proc.). – 2009. – Vol. 28, № 3. – P. 1–6.
3. Becker M. Weakly compressible SPH for free surface flows / M. Becker, M. Teschner // Proc. of the ACM SIGGRAPH/Eurographics Symposium on Computer Animation. – 2007. – P. 209–217.
4. Ihmsen M. Boundary handling and adaptive time-stepping for PCISPH / M. Ihmsen, N. Akinci, M. Gissler, M. Teschner // Proc. of VRIPHYS. – 2010. – P. 79–88.
5. Bodin K. Constraint fluids / K. Bodin, C. Lacoursiere, M. Servin // IEEE Transactions on Visualization and Computer Graphics. – 2012. – Vol. 18. – P. 516–526.
6. Monaghan J. SPH particle boundary forces for arbitrary boundaries / J. Monaghan, J. Kajtar // Computer Physics Communications. – 2009. – Vol. 180, № 10. – P. 1811–1820.
7. Hrytsyshyn O. Application of IISPH for incompressible fluid dynamics simulation / O. Hrytsyshyn, V. Trushevskyy // Вісник Львівського університету. Серія прикладна математика та інформатика. – 2024. – Вип. 33. – С. 55–68.

Article: received 03.9.2025
revised 01.10.2025
printing adoption 15.10.2025

УДОСКОНАЛЕНЕ СЕМПЛЮВАННЯ МЕЖ ДЛЯ МЕТОДУ SPH З ДВОСТОРОННЬОЮ ВЗАЄМОДІЄЮ З ТВЕРДИМИ ТІЛАМИ

О. Грицишин, В. Трушевський

Львівський національний університет імені Івана Франка,
вул. Університетська 1, Львів, 79000, Україна
e-mail: ostap.hrytsyshyn@lnu.edu.ua, valeriy.trushevsky@lnu.edu.ua

Запропоновано практичний підхід до взаємодії рідина–тверде тіло в методі Smoothed Particle Hydrodynamics (SPH). Залишається лише один шар частинок межі, а кожній граничній частинці призначається ефективна маса з поправкою на об'єм. Багатошарові межі можуть давати високу точність, однак на практиці вони важкі: ростуть списки сусідів, збільшується кількість взаємодій, і багато частинок стінки виконують зайву роботу. Ідея одношарового семплювання тримається безпосередньо на поверхні твердого тіла та компенсує відсутніх сусідів локальною оцінкою об'єму V_b, що відображається у $\hat{m}_b = \rho_0 V_b$. Завдяки цій корекції суми для щільності та тиску поблизу стінки залишаються узгодженими навіть для тонких пластин і оболонок, тоді як кількість попарних взаємодій зменшується.

Зв'язування використовує стандартні симетричні сили SPH, тому лінійний та кутовий імпульс зберігаються без штрафів за контакт і без корекцій положення. Інтеграція є простою як у WCSPH (слабкостислива SPH), так і у PCISPH (прогнозно–коригувальна нестислива SPH): додаткові граничні доданки отримує лише підсумовування щільності, тоді як тискові та в'язкі складові зберігають звичну форму. Схема зручна в реалізації, працює з наявним пошуком сусідів і дозволяє керувати ковзанням через типові параметри в'язкості.

Ключові слова: SPH (метод згладжених частинок), взаємодія рідина–тверде тіло, семплювання межі, одношарові межі, об'ємна корекція, дефіцит частинок, моделювання в реальному часі.